THE JOURNAL OF PHYSICAL CHEMISTRY C

Article

pubs.acs.org/JPCC

# Peculiar Piezoelectric Properties of Soft Two-Dimensional Materials

Cem Sevik,*[,†] Deniz Çakır,*[,‡] Oğuz Gülseren,*[,§] and François M. Peeters*[,‡]

[†]Department of Mechanical Engineering, Faculty of Engineering, Anadolu University, Eskisehir, TR 26555, Turkey

[‡]Department of Physics, University of Antwerp, Groenenborgerlaan 171, B-2020 Antwerpen, Belgium

[§]Department of Physics, Bilkent University, Bilkent, Ankara 06800, Turkey

**ABSTRACT:** Group II−VI semiconductor honeycomb monolayers have a noncentrosymmetric crystal structure and therefore are expected to be important for nano piezoelectric device applications. This motivated us to perform first-principles calculations based on density functional theory to unveil the piezoelectric properties (i.e., piezoelectric stress ($e_{11}$) and piezoelectric strain ($d_{11}$) coefficients) of these monolayer materials with chemical formula MX (where M = Be, Mg, Ca, Sr, Ba, Zr, Cd and X = S, Se, Te). We found that these two-dimensional materials have peculiar piezoelectric properties with $d_{11}$ coefficients 1 order of magnitude larger than those of commercially utilized bulk materials. A clear trend in their piezoelectric properties emerges, which originates mainly from their mechanical properties. We establish a simple correlation between the piezoelectric strain coefficients and the physical properties, as the natural elemental polarizabilities, the Bader charges, and lattice constants of the individual M/X atoms and MX monolayers.

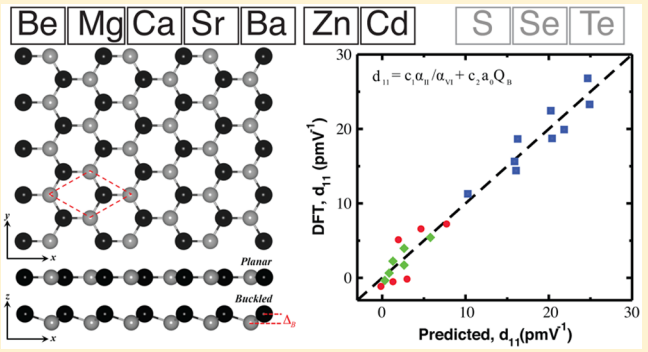


## INTRODUCTION

Recent experimental and theoretical studies revealed that noncentrosymmetric two-dimensional (2D) materials exhibit high piezoelectric responses, which makes them very appealing for the next generation of sensors, actuators, transducers, and energy harvesters. Those applications are in the fields of nanorobotics, piezotronics, and nanoelectromechanical systems.[1−8] The piezoelectric properties of single layer BN, $MoS_2$, $MoSe_2$, $MoTe_2$, $WS_2$, $WSe_2$, and $WTe_2$ were previously studied,[9−12] and it was reported that the relaxed-ion piezoelectric stress ($e_{11}$) and piezoelectric strain ($d_{11}$) coefficients of these monolayers are comparable or even better than those of conventional bulk piezoelectric materials. Likewise, Zhuang et al.[13] have shown that both the $e_{11}$ and $d_{11}$ coefficients of $CrS_2$ are significantly larger than those of single layer $MoS_2$. Subsequently, Wu et al.[1] reported experimental evidence of piezoelectricity in free-standing monolayer $MoS_2$ and they found that this material exhibits a strong piezoelectric effect for an odd number of layers in which case inversion symmetry is broken. Moreover, Zhu et al.[2] measured the $e_{11}$ coefficient of this monolayer material and found $2.9 \times 10^{-10}$ C m$^{-1}$, which is in good agreement with previous theoretical calculation.[9]

Following these studies, the piezoelectric properties of different noncentrosymetric 2D monolayer materials such as transition metal dichalcogenides (TMDCs) and oxides,[14,15] group III monochalcogenides,[16] and group IV monochalcogenides[3,17] were studied by first-principles calculations. Rather surprisingly, the relaxed-ion $d_{11}$ coefficient, which is a measure of the mechanical-electrical energy conversion ratio, of some of these materials was predicted to be 1 or 2 orders of magnitude larger than that of traditionally used bulk materials such as $\alpha$-quartz[18] ($d_{11}$ = 2.3 pm V$^{-1}$), wurtzite-GaN[19] ($d_{33}$ = 3.1 pm V$^{-1}$), and wurtzite-AlN[19] ($d_{33}$ = 5.1 pm V$^{-1}$). For instance, values as high as 8.47, 16.3, 21.7, 212.1, and 250.5 pm V$^{-1}$ have been obtained for monolayer $CrSe_2$, $CrTe_2$,[14] CdO,[15] GeSe, and SnSe[3] crystals, respectively. These results clearly show the remarkably high piezoelectric properties of monolayer materials and their potential use for nanoscale technological applications.

Recently, Zheng et al.[20] explored the structural stability of two-dimensional II−VI honeycomb structures using first-principles lattice-vibration frequency analysis and reported that graphene-like monolayers of BeO, MgO, CaO, ZnO, CdO, CaS, SrS, SrSe, BaTe, and HgTe are dynamically stable. In addition, they confirmed the intrinsic semiconductor nature of these materials by hybrid functional calculations. These results motivated us to perform a systematic first-principles study to investigate piezoelectric and mechanical properties of these noncentrosymmetric single layer materials with chemical formula MX, where M = Be, Mg, Ca, Sr, Ba, Zn, Cd and X = S, Se, Te. Lattice parameters, elastic stiffness constants ($C_{11}$ and $C_{12}$), Young modulus ($Y$), piezoelectric stress coefficients ($e_{11}$) and piezoelectric strain coefficients ($d_{11}$) are calculated.

The present paper is organized as follows. We first present our computational methodology. Then, we calculated the elastic constants and piezoelectric properties. Lastly, we conclude with an overview of our main results.

**Received:** April 7, 2016
**Revised:** June 3, 2016
**Published:** June 9, 2016






DOI: 10.1021/acs.jpcc.6b03543
J. Phys. Chem. C 2016, 120, 13948−13953

## METHOD

Within the scope of the current study, first-principles calculations based on density functional-theory (DFT), as implemented in the Vienna Ab initio Simulation package (VASP) code,[21,22] are performed. The exchange−correlation interactions are treated using the generalized gradient approximation (GGA) within the Perdew−Burke−Ernzerhof (PBE) formulation.[23,24] The single electron wave functions are expanded in plane waves with kinetic energy cutoff of 600 eV. For the structure optimizations, the Brillouin-zone integrations are performed using a Γ-centered regular 26 × 26 × 1 $k$-point mesh within the Monkhorst−Pack scheme.[25] The convergence criterion for electronic and ionic relaxations are set as $10^{-7}$ and $10^{-3}$ eV/Å, respectively. To minimize the periodic interaction along the $z$-direction, the vacuum space between the layers is taken at least 15 Å. The coefficients of elastic stiffness tensor and piezoelectric tensor, $e_{ijk}$ are obtained by using density-functional perturbation theory (DFPT)[26] as implemented in the VASP code. Here, a highly dense $k$-point mesh, 36 × 36 × 1, is used to accurately predict these tensor components. The clamped-ion elastic and piezoelectric coefficients are obtained from the purely electronic contribution and the relaxed-ion coefficients are obtained from the sum of ionic and electronic contributions.

The number of independent piezoelectric tensor coefficient is deduced from the symmetry of the crystal. Due to the symmetry, we only have a non-vanishing piezoelectric effect along the armchair direction for planar structures. The piezoelectric constants are zero for the zigzag direction since this material family is centrosymmetric along the zigzag direction. Thus, the piezoelectric tensor of these hexagonal crystal systems, schematically shown in Figure 1 becomes:

$$e_{ij} = \begin{pmatrix} e_{11} & -e_{11} & 0 \\ 0 & 0 & -\frac{e_{11}}{2} \\ e_{31} & e_{31} & 0 \end{pmatrix} \quad (1)$$

Here, we only need to calculate the $e_{11}$ component of the piezoelectric stress tensor. The piezoelectric coefficient $e_{31}$ is only relevant for a buckled monolayer. Because the calculated $e_{31}$ and $d_{31}$ coefficients are quite small, we are only interested in the in-plane piezoelectric properties. Following the $e_{11}$ calculations, the corresponding piezoelectric strain tensor ($d_{11}$) of each material is predicted from the following relation as previously shown by Duerloo et al.[9]

$$d_{11} = e_{11}/(C_{11} - C_{12}) \quad (2)$$

## RESULTS

It is essential that a piezoelectric material has to be an insulator or semiconductor with a sufficiently wide band gap to avoid current leakage. Zheng et al.[20] confirmed the intrinsic semiconductor nature of the materials considered in this study by hybrid functional calculations. They estimated indirect band gap values of MX with M = Be, Mg, Ca, Sr, Ba and direct band gap values of MX with M = Zn and Cd as large as 2 eV, which are sufficiently large for piezoelectric applications.

With the intention to investigate piezoelectric properties of these materials, we first optimize the geometries and calculate the relaxed- and clamped-ion elastic stiffness coefficients ($C_{11}$ and $C_{12}$), Young's moduli ($Y = (C_{11}^2 - C_{12}^2)/C_{11}$), and Poisson ratios ($\nu = C_{12}/C_{11}$) of all the materials, as depicted in Table 1. Because local density approximation was used in ref 20, we obtain slightly larger equilibrium lattice constants. The calculated buckling parameters, $\Delta_B$ (Figure 1), for nonplanar structures are 0.21, 0.41, 0.32, and 0.49 Å for ZnSe, ZnTe, CdSe, and CdTe, respectively. The first observation from Table 1 is that $C_{11}$, $C_{12}$, $Y$, and $\nu$ of group II−VI materials decreases with an increase in the row number of the group II element. In addition, for each group II element, the MX monolayer becomes stiffer with an increase in the row number of the group VI element. Note that the relaxed-ion elastic constants, i.e., $C_{11}$ and $C_{12}$, are mostly smaller than the clamped-ion ones because the internal relaxation of the ions allows the release of some of the stress in the former, Table 1. All the materials considered in this study are found to be less stiff when compared to graphene ($Y$ = 341 N/m),[27] single layer $h$-BN ($Y$ = 275.9 N/m),[27] and most of the TMDCs,[14] and the Poisson ratios, $\nu$, of most of the MX compounds are much larger than that of TMDCs.[27] On the contrary, it should be noticed that the calculated elastic constants are positive and satisfy the Born stability criteria for crystals having hexagonal symmetry (for which the following conditions must be met for mechanically stable hexagonal crystals: $C_{11} > |C_{12}|$ and $C_{11} > 0$).[28,29]

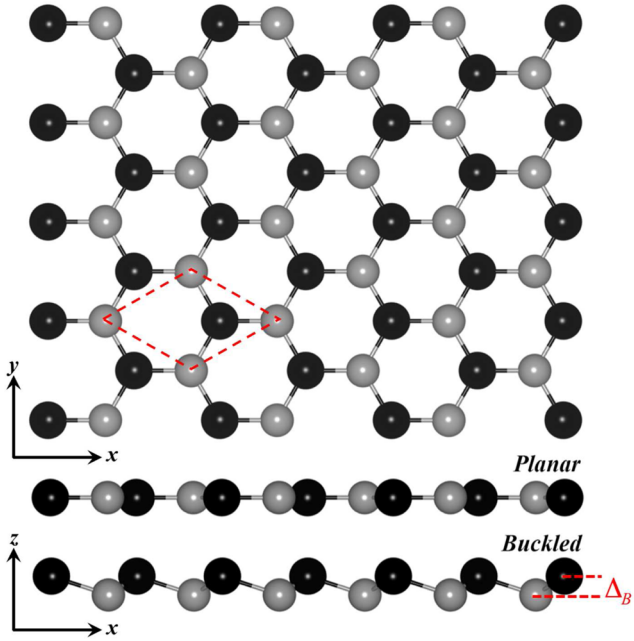


**Figure 1.** Top and side views of graphene-like honeycomb structure for group II−VI MX monolayers, where M = Be, Mg, Ca, Sr, Ba, Zr, Cd and X = S, Se, Te. $\Delta_B$ is the buckling parameter for the nonplanar monolayers.

Figure 2 shows the results for clamped-ion (purely electronic) and relaxed-ion (electronic plus ionic) $e_{11}$ and $d_{11}$ coefficients of MX structures with M = Be, Mg, Ca, Sr, Ba and X = S, Se, Te. The calculated values clearly show that the electronic and ionic polarization of these materials have opposite sign and the magnitude of the ionic contribution is larger than the electronic contribution for all the considered materials except those with Be atom.

The contribution of the internal relaxation to the relaxed-ion $e_{11}$ coefficients decreases when moving downward in the group of chalcogenide atoms. Owing to their larger in-plane lattice parameters, the MX compounds with larger M and X atoms undergo a smaller internal relaxation, which reduces the ionic


DOI: 10.1021/acs.jpcc.6b03543
J. Phys. Chem. C 2016, 120, 13948−13953

Table 1. Calculated Equilibrium Lattice Constants $a_0$ (Å), Net Bader Charge Q on the Metal Atoms ($e^-$), Electronegativity Difference ($\Delta\chi = \chi_X - \chi_M$) of M and X Atoms (in Pauling Scale), Clamped- and Relaxed-Ion Elastic Constants $C_{11}$ and $C_{12}$ (N/m), the Young Modulus $Y$ (N/m), and the Poisson Ratios $\nu$ ($=C_{12}/C_{11}$)

| | | | | clamped | | | | relaxed | | | |
|---|---|---|---|---|---|---|---|---|---|---|---|
| material | $a_0$ | Q | $\Delta\chi$ | $C_{11}$ | $C_{12}$ | Y | $\nu$ | $C_{11}$ | $C_{12}$ | Y | $\nu$ |
| BeS | 3.456 | 1.59 | 1.01 | 87 | 22 | 81 | 0.25 | 78 | 31 | 65 | 0.40 |
| BeSe | 3.671 | 1.55 | 0.98 | 75 | 19 | 70 | 0.25 | 67 | 26 | 57 | 0.39 |
| BeTe | 4.033 | 1.45 | 0.53 | 61 | 14 | 57 | 0.23 | 54 | 21 | 46 | 0.39 |
| MgS | 4.095 | 1.68 | 1.27 | 56 | 18 | 49 | 0.32 | 45 | 29 | 26 | 0.64 |
| MgSe | 4.308 | 1.60 | 1.24 | 48 | 16 | 42 | 0.33 | 39 | 25 | 23 | 0.64 |
| MgTe | 4.684 | 1.54 | 0.79 | 38 | 13 | 34 | 0.34 | 31 | 20 | 19 | 0.65 |
| CaS | 4.572 | 1.45 | 1.58 | 39 | 18 | 32 | 0.46 | 32 | 25 | 12 | 0.78 |
| CaSe | 4.780 | 1.44 | 1.55 | 35 | 15 | 28 | 0.43 | 27 | 22 | 9 | 0.81 |
| CaTe | 5.160 | 1.43 | 1.10 | 29 | 12 | 23 | 0.41 | 22 | 19 | 7 | 0.86 |
| SrS | 4.849 | 1.50 | 1.63 | 35 | 16 | 28 | 0.46 | 28 | 23 | 10 | 0.82 |
| SrSe | 5.058 | 1.48 | 1.60 | 31 | 14 | 25 | 0.45 | 24 | 20 | 8 | 0.83 |
| SrTe | 5.438 | 1.43 | 1.15 | 26 | 11 | 21 | 0.42 | 20 | 17 | 6 | 0.85 |
| BaS | 5.140 | 1.42 | 1.69 | 30 | 16 | 22 | 0.53 | 25 | 21 | 8 | 0.84 |
| BaSe | 5.350 | 1.39 | 1.66 | 27 | 14 | 20 | 0.52 | 22 | 18 | 7 | 0.82 |
| BaTe | 5.728 | 1.36 | 1.21 | 23 | 11 | 17 | 0.48 | 18 | 16 | 5 | 0.89 |
| ZnS | 3.892 | 0.95 | 0.93 | 70 | 19 | 64 | 0.27 | 59 | 30 | 44 | 0.51 |
| ZnSe | 4.097 | 0.74 | 0.90 | 58 | 16 | 54 | 0.28 | 40 | 15 | 34 | 0.38 |
| ZnTe | 4.404 | 0.50 | 0.45 | 47 | 13 | 43 | 0.28 | 34 | 13 | 29 | 0.38 |
| CdS | 4.258 | 0.90 | 0.89 | 56 | 18 | 50 | 0.32 | 46 | 28 | 28 | 0.61 |
| CdSe | 4.440 | 0.73 | 0.86 | 47 | 15 | 42 | 0.32 | 30 | 15 | 23 | 0.50 |
| CdTe | 4.723 | 0.52 | 0.41 | 39 | 12 | 35 | 0.31 | 25 | 11 | 20 | 0.44 |

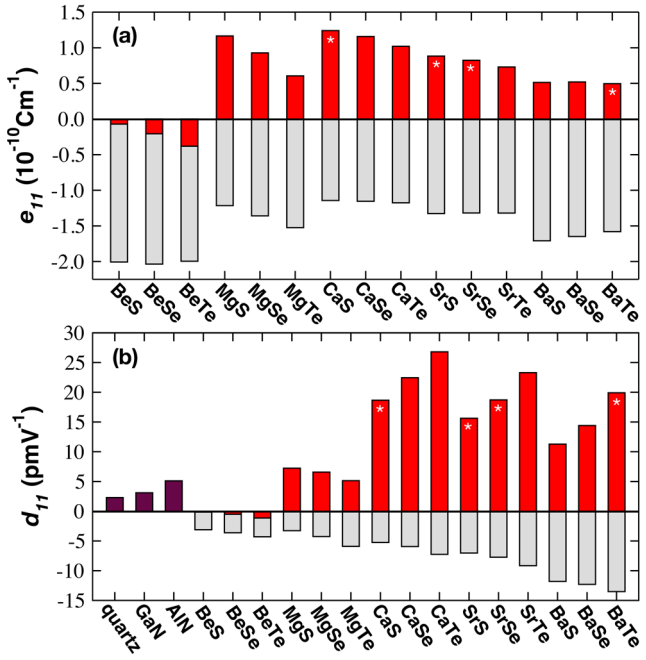


**Figure 2.** Calculated clamped- and relaxed-ion (a) piezoelectric stress ($e_{11}$) and (b) piezoelectric strain ($d_{11}$) coefficients for MX monolayers (where M = Be, Mg, Ca, Sr, and Ba). Red (gray) bars depict the relaxed-ion (clamped-ion) piezoelectric coefficients. For comparison, $d_{11}$ coefficient of $\alpha$-quartz, GaN, and AlN are also depicted in (b). The white asterisk indicates that it is a dynamically stable material.

contribution. This may be due to the fact that MX compounds possessing large cell parameters have a very smooth potential energy surface. Thus, moving slightly away from the equilibrium structure does not change the total energy of the system. Although the clamped-ion $e_{11}$ coefficients in the Ba-based compounds are larger than that in most of the group II elements, the relaxed-ion $e_{11}$ coefficients exhibit a opposite behavior.

Among MX materials, MgS, CaS, and CaSe have the highest and BeS has the smallest relaxed-ion $e_{11}$ coefficients, as seen in Figure 2a. Moreover, the predicted highest $e_{11}$ coefficient is smaller than the one calculated for $WS_2$ (3.76,[14] 2.47,[9] and 2.12[15]), which has the smallest relaxed-ion coefficient among the Cr, Mo, and W based transition metal dichalcogenides (TMDCs). However, the picture is completely different when we consider the relaxed-ion $d_{11}$ coefficient, which is a measure of the mechanical-electrical energy conversion ratio, Figure 2b. In particular, the ones calculated for MX with M = Ca, Sr, and Ba are notably larger than the values predicted for TMDCs,[9,14,15] most of the monolayer materials such as BN, GaSe, GaAs, and AlSb,[3,20] and the bulk materials including $\alpha$-quartz, wurtzite-GaN, and wurtzite-AlN,[18,19] which are widely used in industry. Furthermore, the materials previously reported as having good dynamic stability, namely, CaS, SrS, SrSe, and BaTe,[20] have appreciable $d_{11}$ coefficients with values of 18.66, 15.64, 18.73, and 19.92 pm V$^{-1}$, respectively.

As clearly understood from eq 2, such a remarkable $d_{11}$ coefficient is obviously correlated to the mechanical properties of the structures because these materials possess quite similar $e_{11}$ coefficients; see elastic stiffness coefficients and Young's moduli listed in Table 1. This explicitly indicates that, in this material class, the remarkable piezoelectric potential originates mainly from their mechanical responses. Although the relaxed-ion $e_{11}$ coefficients of MX materials span a limited range (0.07−1.24 pC/m), the absolute values of the relaxed-ion $d_{11}$ coefficient vary over a much larger range of 0.15−27 pm/V.

Though the relaxed-ion $e_{11}$ coefficient decreases when going from S to Te for all group II elements, the relaxed-ion $d_{11}$ coefficient follows a different trend such that it increases when moving downward in the group of chalcogenides for the Ca, Sr


DOI: 10.1021/acs.jpcc.6b03543
J. Phys. Chem. C 2016, 120, 13948−13953

and Ba atoms. BeX and MgX compounds have relatively large electronegativity difference, which is expected to result in large relaxed-ion $d_{11}$ coefficients. However, due to their larger stiffness, the relaxed-ion $d_{11}$ coefficients of the BeX and MgX compounds are found to be significantly smaller than that of MX with M = Ca, Sr, and Ba but are comparable with those of commercial piezoelectric materials, Figure 2b. Here it should be mentioned that, among TMDCs with M = Cr, Mo, and W, $CrTe_2$ has the largest $d_{11}$ coefficient whereas BeTe has one of the smallest $d_{11}$ coefficient among MX materials considered in this work.

In addition to Be, Mg, Ca, Sr, and Ba we also considered Zn and Cd based structures as well. Figure 3 shows the calculated

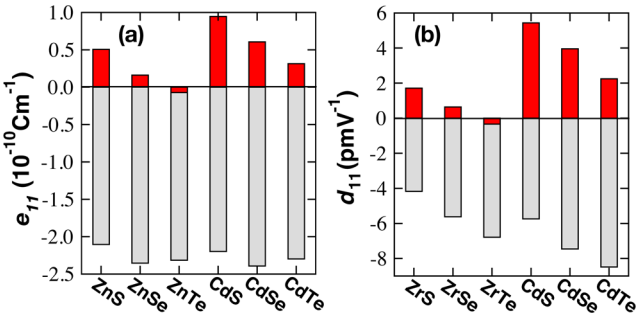


**Figure 3.** Calculated clamped- and relaxed-ion (a) piezoelectric stress ($e_{11}$) and (b) piezoelectric strain ($d_{11}$) coefficients for the MX monolayers (where M = Zr and Cd). Red (gray) bars depict the relaxed-ion (clamped-ion) piezoelectric coefficients.

$e_{11}$ and $d_{11}$ coefficients for ZnX, and CdX with X = S, Se, and Te. The relaxed-ion $e_{11}$ coefficients of the MX materials (with M = Zn and Cd) fall into the range 0.07−0.94 pC/m and are comparable to those of the MX materials (with M = Be, Mg, Ca, Sr, and Ba) but much smaller than the $e_{11}$ coefficients of TMDCs. Furthermore, the clamped-ion $e_{11}$ coefficients are quite similar for the ZnX and CdX compounds. This means that the ionic contribution determines the trends found for the relaxed-ion $e_{11}$ coefficients, Figure 3a. Because the MX compounds are remarkably less stiff than the TMDCs, the predicted $d_{11}$ coefficients of MX materials are comparable with that of TMDCs. In contrast to CaX, SrX, and BaX, the relaxed-ion $d_{11}$ coefficients of ZnX and CdX decrease when moving from S to Te. Similar trends also hold for MgX. In addition, CdX compounds have much larger $d_{11}$ coefficients with respect to ZnX. Considering electronegativity differences between Zn/Cd and X atoms (which can be used to determine bond type in a material), the ZnX/CdX compounds with X = Te (S) belongs to a nonpolar covalent (polar covalent) bond class rather than a polar covalent (nonpolar covalent) bond class, which can be understood by comparing their Bader charges and electronegativity differences given in Table 1. Thus, we can claim that the larger the electronegativity difference, the larger the $d_{11}$ coefficient is. If one compares elastic constants, ZnX and CdX compounds are stiffer than the group II monochalcogenides. According to eq 2, the $d_{11}$ coefficient is inversely proportional to $(C_{11}-C_{12})$, which is found to be large for ZnX and CdX materials. Even though Te is the most easily polarizable atom among the group VI elements, the relaxed-ion $d_{11}$ coefficients of ZnTe and CdTe are found to be one-third of those of ZnS and CdS.

Compared to TMDC properties, the piezoelectric properties of the MX materials are much more complicated. In the former, $d_{11}$ is only governed by the ratio of the natural elemental polarizabilities of metal and chalcogenide atoms such that the $d_{11}$ coefficient is maximized if we use a smaller metal atom and a larger chalcogenide atom.[14] Finally, we attempt to relate the observed trends in the $d_{11}$ coefficients to some physical properties, such as atomic polarizabilities, Bader charges, lattice constants, etc., of individual atoms and their monolayers. We predict that the $d_{11}$ coefficient of the materials under study are directly proportional to the ratio of natural elemental polarizabilities of M and X atoms and the product of lattice constants and Bader charges, as shown in Figure 4. There is a

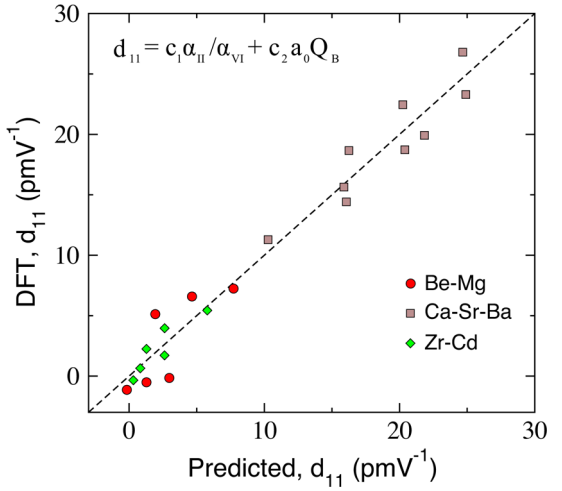


**Figure 4.** Correlation between the relaxed-ion $d_{11}$ coefficients of materials predicted by DFT calculations and the simple formula shown as inset. Here, $\alpha_{II}$ and $\alpha_{VI}$ represent the atomic polarizabilities[30] of the group II and VI atoms and $c_1$ and $c_2$ are constants. The red filled circles, brown filled squares, and green filled diamonds denote the MX monolayers with M = Be−Mg, Ca−Sr−Ba, and Zr−Cd groups, respectively.

very good correlation between the coefficients calculated with the simple formula, $d_{11} = c_1\frac{\alpha_{II}}{\alpha_{VI}} + c_2 a_0 Q_B$ and the DFPT calculations.[15] Here, the natural elemental polarizabilities are borrowed from the experimental and calculated static dipole polarizabilities for the electronic ground states of neutral elements.[30] $a_0$ is the lattice constant and $Q_B$ is the Bader charge given for the metal atoms (i.e., Be, Mg, Ca, Sr, Ba, Zr, Cd) in Table 1. $c_1$ and $c_2$ are fitting constants shown in Table 2. In this

**Table 2. Correlation Coefficients for the Simple Formula, $d_{11} = c_1\frac{\alpha_{II}}{\alpha_{VI}} + c_2 a_0 Q_B$**

| materials[a] | $c_1$ | $c_2$ |
|---|---|---|
| BeX, MgX | 3.2295 | −0.5501 |
| CaX, SrX, BaX | −1.4305 | 4.1700 |
| ZnX, CdX | 9.6994 | −4.4837 |

[a]Here, X represents S, Se, and Te atoms.

equation, the second term is a kind of dipole moment scaled with a constant (i.e., $c_2$). Hence, it is possible to predict the piezoelectric constants without doing expensive calculations just by knowing tabulated atomic polarizabilities, the Bader charges (or electronegativities) and lattice parameters. Due to differences in mechanical properties of MX monolayers and electronic properties of individual M and X atoms, we identify


DOI: 10.1021/acs.jpcc.6b03543
J. Phys. Chem. C 2016, 120, 13948−13953

three sets of fitting parameters that are exactly the same within the groups of Be−Mg, Ca−Sr−Ba, and Zn−Cd. In each fitting group, $c_1$ and $c_2$ parameters have opposite signs. According to this simple formula, there is a correlation between the $d_{11}$ coefficient and the Bader charges. This simple expression also indicates that the $d_{11}$ coefficient is maximized if one considers a smaller metal atom and a larger chalcogenide atom as we show for Ca, Sr, and Be.

## CONCLUSION

We presented a detailed theoretical investigation of the piezoelectric properties of semiconducting two-dimensional MX (where M = Be, Mg, Ca, Sr, Ba, Zr, Cd and X = S, Se, Te) monolayers. These structures are found to be strong candidates for future atomically thin piezoelectric applications. Due to their mechanical softness, MX monolayers have a surprisingly very high relaxed-ion $d_{11}$ coefficient. We showed that most of these materials have much better piezoelectric properties than most of the other two-dimensional materials and the well-known conventional bulk piezoelectric materials. Notable MX monolayers with good stability and high relaxed-ion $d_{11}$ coefficient include BaTe (19.92 pm/V), SrSe (18.73 pm/V), SrS (15.64 pm/V), and CaS (18.66 pm/V). In addition, we noticed that it is possible to relate the calculated relaxed-ion $d_{11}$ coefficients with atomic polarizabilities and the Bader charges of M and X atoms, and the structural properties of MX monolayers. The calculated relaxed-ion $d_{11}$ coefficients can be fitted to a linear combination of two terms, the ratio of the M and X polarizabilities and the product of the Bader charges and in-plane lattice constants.

## AUTHOR INFORMATION


### Corresponding Authors

*C. Sevik. E-mail: csevik@anadolu.edu.tr. Phone: +9 (0)532 1673208.
*D. Çakır. E-mail: deniz.cakir@uantwerpen.be.
*O. Gülseren. E-mail: gulseren@fen.bilkent.edu.tr.
*F. Peeters. E-mail: francois.peeters@uantwerpen.be.


### Notes

The authors declare no competing financial interest.

## ACKNOWLEDGMENTS

This work was supported by the Flemish Science Foundation (FWO-Vl), the Methusalem foundation of the Flemish government and the Bilateral program FWO-TUBITAK between Flanders and Turkey. We acknowledge the support from the Scientific and Technological Research Council of Turkey (TUBITAK-115F024). Computational resources were provided by TUBITAK ULAKBIM, High Performance and Grid Computing Center (TR-Grid e-Infrastructure), and HPC infrastructure of the University of Antwerp (Cal-cUA) a division of the Flemish Supercomputer Center (VSC), which is funded by the Hercules foundation. C.S. acknowledges the support from the Scientific and Technological Research Council of Turkey (TUBITAK-113F333) and the support from Anadolu University (BAP-1407F335, -1505F200), and the Turkish Academy of Sciences (TUBA-GEBIP).

## REFERENCES


(1) Wu, W.; Wang, L.; Li, Y.; Zhang, F.; Lin, L.; Niu, S.; Chenet, D.; Zhang, X.; Hao, Y.; Heinz, T. F.; et al. Piezoelectricity of Single-Atomic-Layer $MoS_2$ for Energy Conversion and Piezotronics. *Nature* **2014**, *514*, 470−474.
(2) Zhu, H.; Wang, Y.; Xiao, J.; Liu, M.; Xiong, S.; Wong, Z. J.; Ye, Z.; Ye, Y.; Yin, X.; Zhang, X. Observation of Piezoelectricity in Free-Standing Monolayer $MoS_2$. *Nat. Nanotechnol.* **2015**, *10*, 151−155.
(3) Fei, R.; Li, W.; Li, J.; Yang, L. Giant Piezoelectricity of Monolayer Group IV Monochalcogenides: SnSe, SnS, GeSe, and GeS. *Appl. Phys. Lett.* **2015**, *107*, 173104−173108.
(4) Ong, M. T.; Reed, E. J. Engineered Piezoelectricity in Graphene. *ACS Nano* **2012**, *6*, 1387−1394.
(5) Kaul, A. B.; Wong, E. W.; Epp, L.; Hunt, B. D. Electromechanical Carbon Nanotube Switches for High-Frequency Applications. *Nano Lett.* **2006**, *6*, 942−947.
(6) Zhang, C.; Chen, W.; Zhang, C. Two-dimensional Theory of Piezoelectric Plates Considering Surface Effect. *Eur. J. Mech. A-Solid* **2013**, *41*, 50−57.
(7) Kim, K.-H.; Kumar, B.; Lee, K. Y.; Park, H.-K.; Lee, J.-H.; Lee, H. H.; Jun, H.; Lee, D.; Kim, S.-W. Piezoelectric two-dimensional nanosheets/anionic layer heterojunction for efficient direct current power generation. *Sci. Rep.* **2013**, *3*, 2017 EP.
(8) Lanza, M.; Reguant, M.; Zou, G.; Lv, P.; Li, H.; Chin, R.; Liang, H.; Yu, D.; Zhang, Y.; Liu, Z.; et al. High-Performance Piezoelectric Nanogenerators Using Two-Dimensional Flexible Top Electrodes. *Adv. Mater. Interfaces* **2014**, *1*, 1300101.
(9) Duerloo, K. A. N.; Ong, M. T.; Reed, E. J. Intrinsic Piezoelectricity in Two-Dimensional Materials. *J. Phys. Chem. Lett.* **2012**, *3*, 2871−2876.
(10) Michel, K. H.; Verberck, B. Theory of Elastic and Piezoelectric Effects in Two-Dimensional Hexagonal Boron Nitride. *Phys. Rev. B: Condens. Matter Mater. Phys.* **2009**, *80*, 224301.
(11) Michel, K. H.; Verberck, B. Phonon Dispersions and Piezoelectricity in Bulk and Multilayers of Hexagonal Boron Nitride. *Phys. Rev. B: Condens. Matter Mater. Phys.* **2011**, *83*, 115328.
(12) Michel, K. H.; Verberck, B. Theory of Phonon Dispersions and Piezoelectricity in Multilayers of Hexagonal Boron-Nitride. *Phys. Status Solidi B* **2011**, *248*, 2720.
(13) Zhuang, H. L.; Johannes, M. D.; Blonsky, M. N.; Hennig, R. G. Computational Prediction and Characterization of Single-Layer $CrS_2$. *Appl. Phys. Lett.* **2014**, *104*, 022116−022119.
(14) Alyörük, M. M.; Aierken, Y.; Çakır, D.; Peeters, F. M.; Sevik, C. Promising Piezoelectric Performance of Single Layer Transition-Metal Dichalcogenides and Dioxides. *J. Phys. Chem. C* **2015**, *119*, 23231−23237.
(15) Blonsky, M. N.; Zhuang, H. L.; Singh, A. K.; Hennig, R. G. Ab Initio Prediction of Piezoelectricity in Two-Dimensional Materials. *ACS Nano* **2015**, *9*, 9885−9891.
(16) Li, W.; Li, J. Piezoelectricity in Two-Dimensional Group-III Monochalcogenides. *Nano Res.* **2015**, *8*, 3796−3802.
(17) Gomes, L. C.; Carvalho, A.; Castro Neto, A. H. Enhanced Piezoelectricity and Modified Dielectric Screening of Two-Dimensional Group-IV Monochalcogenides. *Phys. Rev. B: Condens. Matter Mater. Phys.* **2015**, *92*, 214103.
(18) Behmann, R. Elastic and Piezoelectric Constants of alpha-Quartz. *Phys. Rev.* **1958**, *110*, 1060−1061.
(19) Lueng, C. M.; Chan, H. L. W.; Surya, C.; Choy, C. L. Piezoelectric Coefficient of Aluminum Nitride and Gallium Nitride. *J. Appl. Phys.* **2000**, *88*, 5360−5363.
(20) Zheng, H.; Li, X.-B.; Chen, N.-K.; Xie, S.-Y.; Tian, W. Q.; Chen, Y.; Xia, H.; Zhang, S. B.; Sun, H.-B. Monolayer II-VI Semiconductors: A First-Principles Prediction. *Phys. Rev. B: Condens. Matter Mater. Phys.* **2015**, *92*, 115307.
(21) Kresse, G.; Hafner, J. Ab Initio Molecular Dynamics for Liquid Metals. *Phys. Rev. B: Condens. Matter Mater. Phys.* **1993**, *47*, 558−561.
(22) Wu, X.; Vanderbilt, D.; Hamann, D. R. Systematic Treatment of Displacements, Strains, And Electric Fields in Density-Functional Perturbation Theory. *Phys. Rev. B: Condens. Matter Mater. Phys.* **2005**, *72*, 035105.
(23) Perdew, J. P.; Burke, K.; Ernzerhof, M. Generalized Gradient Approximation Made Simple. *Phys. Rev. Lett.* **1996**, *77*, 3865−3868.



DOI: 10.1021/acs.jpcc.6b03543
J. Phys. Chem. C 2016, 120, 13948−13953

(24) Perdew, J. P.; Burke, K.; Ernzerhof, M. Generalized Gradient Approximation Made Simple. *Phys. Rev. Lett.* **1996**, *77*, 3865−3868.
(25) Monkhorst, H. J.; Pack, J. D. Special Points for Brillouin-Zone Integrations. *Phys. Rev. B* **1976**, *13*, 5188−5192.
(26) Nunes, R. W.; Gonze, X. Berry-Phase Treatment of the Homogeneous Electric Field Perturbation in Insulators. *Phys. Rev. B: Condens. Matter Mater. Phys.* **2001**, *63*, 155107.
(27) Çakır, D.; Peeters, F. M.; Sevik, C. Mechanical and Thermal Properties of *h*-$MX_2$ Monolayers a Comparative Study. *Appl. Phys. Lett.* **2014**, *104*, 203110−203113.
(28) Born, M.; Huang, K. *Dynamical Theory of Crystal Lattices*; Oxford University Press: Oxford, U.K., 1988.
(29) Nye, J. F. *Physical Properties of Crystals, Their Representation by Tensors and Matrices*; Clarendon Press: Oxford, U.K., 1957.
(30) Schwerdtfeger, P. Table of Experimental and Calculated Static Dipole Polarizabilities for the Electronic Ground States of the Neutral Elements (in Atomic Units): http://ctcp.massey.ac.nz/Tablepol2015.pdf. 2015, $\alpha_{Be}$/37.71, $\alpha_{Mg}$/70.89, $\alpha_{Ca}$/155.90, $\alpha_{Sr}$/197.20, $\alpha_{Ba}$/275.68, $\alpha_{Zn}$/38.80, $\alpha_{Cd}$/46.60, $\alpha_{S}$/19.60, $\alpha_{Se}$/26.24, $\alpha_{Te}$/37.00.



DOI: 10.1021/acs.jpcc.6b03543
*J. Phys. Chem. C* 2016, 120, 13948−13953